Internal circulation within the liquid slugs of liquid-liquid slug flow capillary microreactor

M. N. Kashid[1,2,*], I. Gerlach[1], S. Goetz[3], J. Franzke[4], J. F. Acker[2], F. Platte[1,2], D. W. Agar[1] and S. Turek[2]

[1] Institute of Reaction Engineering, University of Dortmund, 44227 Dortmund, Germany.

[2] Institute for Applied Mathematics, University of Dortmund, 44227 Dortmund, Germany.

[3] Chair of Energy Process Engineering and Fluid Mechanics, University of Dortmund, 44227 Dortmund, Germany.

[4] ISAS - Institute for Analytical Sciences, 44139 Dortmund, Germany

Abstract

A so-called "slug flow" capillary microreactor has been proposed for the investigation of mass transfer limited liquid-liquid reactions. Internal circulation within the slug leads to an intensified and tunable mass transfer. Understanding the development of the circulatory flows and the influence of operating parameters upon them is thus crucial. In this study, the experiments were carried out to visualise the internal circulations using Particle Image Velocimetry (PIV) technique. Also it uses the state-of-the-art computational fluid dynamics (CFD) simulations to predict the internal circulation within the liquid slugs and a CFD particle tracing algorithm to visualise them. Each slug was modelled as a distinct single-phase flow domain. The effect of flow velocity and slug length on the velocity profile and stagnant zones of the internal circulations for a slug with and without a wall film is discussed. The internal circulations could be qualitatively and quantitatively characterised with the help of the PIV measurements and particle tracing algorithm.

Keywords: Slug Flow, PIV, CFD, Internal Recirculation, Particle Tracing

*Author to whom correspondence should be addressed:
kashid@math.uni-dortmund.de
Tel: + 49 231 755 3453 Fax: + 49 231 755 5933

Introduction

Microreactor technology, an important method of process intensification, offers numerous potential benefits for the process industries. Liquid-liquid reactions with mass transfer limitations may be carried out advantageously on a small-scale in liquid-liquid slug flow microreactor (Burns and Ramshaw[1]; Dummann et al.[2]). In this type of reactor, alternating uniform slugs of the two-phase reaction mixture exhibit well-defined interphase mass transfer areas and flow patterns. The improved control of strongly exothermic and hazardous reactions available is also of technical relevance for large scale production reactors. Two basic mass transfer mechanisms arise: convection within the individual liquid slugs and diffusion between adjacent slugs. The mass transfer is intensified through internal circulation caused by the shear between continuous phase/wall surface and slug axis, which enhances diffusive penetration and consequently increases observed reaction rates. The internal circulatory flow patterns within the slug thus play a decisive role in determining the performance of the reactor as reflected in such parameters as the reaction selectivity, pressure drop and stability of the slug flow regime.

Several experimental and modelling studies have been carried out to identify the hydrodynamic flow regimes and their transitions for gas-liquid flows through various small-scale geometries (Paglianti et al.[3]; Mishima and Hibiki[4]; Triplett et al.[5]; Kreutzer[6] and Simmons et al.[7]). Dispersion and mass transfer studies for gas-liquid flows have also been published (Thulasidas et al.[8]; Bercic and Pinter[9]; Elperin and Fominykh[10] and Van Baten and Krishna[11]). The recent experimental technique, PIV has shown strong potential in flow field measurements (for example, Meinhart et al.[12]; Pan et al.[13]; etc.). The PIV technique was used to establish the flow patterns within the liquid slugs of bubble train flow inside the capillaries by Thulasidas et al.[14] and shown to exhibit circulation patterns with a high degree of internal mixing. A few studies (Piarah et al[15]; Waheed et al.[16]; and Bothe et al.[17]) have addressed the

mass transfer from drops and bubbles to the surrounding fluid and provide numerical algorithms to predict the mass transfer occurring. Recently, Taha and Cui[18] used the volume-of-fluid CFD method to obtain the velocity and bubble profiles for a vertical gas-liquid slug flow inside capillaries and found good agreement with published experimental measurements.

The use of slugs (capsules) in oil transportation was studied experimentally by Hodgson and Charles[19], who reported flow regimes, slug velocities and pressure gradient for oil-water flow through a 1.04 inch diameter horizontal pipe. Using snapshots of flow patterns they revealed that the viscous or semi-rigid oil phase had been completely surrounded by less viscous water. Further, measurements of slug velocity and pressure gradient for laminar and turbulent flow conditions was deduced by Charles[20] with a suitable model. Three decades later this flow scheme was exploited for reaction engineering applications by Professor Ramshaw's group from University of Newcastle. They developed a multiphase microreactor based upon the use of liquid-liquid slug flow and obtained mass transfer performance data for extraction of acetic acid from kerosene slugs (Burns and Ramshaw[1]). During the same period, Dummann et al.[2] carried out experiments for the production of nitrobenzene in a capillary microreactor using the same concept. The reaction was carried out in slug flow regime and focused on reducing the formation of by-products. Some CFD simulations were carried out, leading to the conclusion that the enhancement of mass transfer can be interpreted in terms of an internal circulation flow within the plugs. Recently, Harries et al.[21] developed a numerical model with general purpose CFD code and predicted internal flow patterns of slugs (which they referred as "fluid segments") and the transfer of dissolved chemical species within slugs and across interfaces.

From the literature review, it can be seen that the circulations within the slug are not completely understood and require systematic experimental study and development of refined

models as well. PIV is the flow field measurements technique which can help in better understanding of the flow patterns. In addition, the potential of CFD in revealing details of flows decisive for the performance of chemical reactors has been described in the literature (for example, Ranade[22]; Jiang et al.[23]). In this present work, an attempt has been made to carry out PIV experiments and CFD simulations. The effect of a wall film and other operating parameters like flow velocity and slug length on internal circulations by CFD simulation is discussed. The location and extent of stagnation zones in the slug and characteristic circulation times were calculated from simulated results. For better physical understanding and visualisation, a CFD particle tracing algorithm was developed.

Internal Circulations

The liquid-liquid slug flow in a capillary microreactor is shown in Figure 1a. When these slugs move through the capillary, depending on the prevalent physical properties and operating conditions, internal circulations within the slugs arise. The shear between the wall surface and slug axis produces internal circulations within the slug which reduce the thickness of boundary layer at the phase interface thereby enhances the diffusive penetration. These circulations are illustrated schematically in Figure 1b and show two zones: a recirculation zone at the centre of the slug and a stagnant zone where the liquid velocity is effectively zero. Similar type of circulation inside liquid slug for bubble train flow has been reported by Gruber[24].

Further experimental studies carried out at our laboratory unexpectedly revealed the presence of an organic wall film (~ $0.1R_s$) surrounding the aqueous slug due to superior wetting properties for the capillary wall material (Teflon). The same effect of film formation was observed (Figure 1c) during the lab on chip experiments which are discussed in the following section. The significance of the film is that the whole slug surface takes part in the mass

transfer thus increasing the mass exchange between two phases. The circulation within the slug with film thus exhibits a wall film zone in addition to the recirculation and stagnant zone. In this case, the liquid inside the slug is driven by the outer flow of wall film and slug displacement by enclosed slug. This wall film is not stagnant since the liquid exerts considerable shear stress on it, which keeps the film moving at a low velocity. However, the aqueous slug moves with a velocity slightly greater than the average flow velocity. This velocity can be calculated by assuming a fully developed laminar velocity profile in the capillary (Charles[20]). The velocity of the slug (V_s) is considered as maximum velocity (plug flow behaviour) inside the capillary, and relates average velocity (V_{av}) inside the capillary by the following equation:

$$V_s = \frac{2}{1+(R_s/R)^2} V_{av} \quad (1)$$

Where R is the capillary radius and R_s is the radius of fast moving slug which depends on the wall film thickness (h). This in turn can be represented as a function of the capillary number (ratio of viscous forces and surface tension forces) according to the Bretherton law (Bico and Quere[25]):

$$h = 1.34 R Ca^{2/3} \quad (2)$$

This calculation yields a film thickness approximately equal to the experimentally observed value. For the regulation of the mixing quality of such a slug flow reactor, the exact knowledge of the internal circulations as a function of the average flow rate is necessary. Thulasidas et al[14] defined the circulation time in bubble train flow as time for the liquid to move form one end of the slug to the other end. Analogously, in liquid-liquid slug flow, the dimensionless recirculation time for slugs without film can be written as follows:

$$t_{nofilm} = \frac{L\left(r^0\right)^2}{2\frac{L}{V_{av}}\int_0^{r^0} U(r)\,r\,dr} \tag{3}$$

However, the slug which forms film keeps the part of the liquid circulating inside it, changes the denominator term in the above equation. Considering the volumetric throughputs from stagnant zone radial position (r^0) to end of the recirculation (r), the equation for recirculation time can be written as:

$$t_{film} = \frac{L\left(r^0\right)^2}{2\frac{L}{V_s}\int_{r^0}^{r} U(r)\,r\,dr} \tag{4}$$

PIV Experimentation

From the transport phenomenon point of view, it is crucial to establish the recirculation patterns and stagnant zones. We employed the PIV method, a method for determining flow velocities in a two-dimensional measuring plane. Tracer particles are added to the fluid to visualize its flow. With the aid of a strong source of light – usually lasers are applied – a pulsed, two-dimensional light field is generated to illumine the measuring plane. The light that is scattered by the particles within the measuring plane is recorded by a camera as a sequence of frames. The image recording for the PIV data was carried in a Caliper® 42 Microfluidic Workstation which is schematically illustrated in Figure 2. This is a commercial product having a flow controller and an optical observation stand including a microscope (Nikon TE 300 Inverted Microscope) and electronic image recording (Cohu 1300 High Performance Colour CCD Camera).

The slug flow was generated by applying hydrodynamic pressure to a microfluidic glass chip (LabChip NS145) with T-contactor to a capillary width of 70 µm and depth of 12 µm. The LabChip capillary is illuminated as a whole using a mercury arc lamp. A light plane cannot be applied in these measurements, since the thickness of such a plane exceeds the depth of the capillary. The system examined was water-paraffin oil. The commercially available tracer particles (polystyrene microspheres, Sphero™ Fp-0856-2, density = 1.05 g/cm^3) coated with a fluorescing dye (Nile Red, $\lambda_{ex,\,max}$ = 510 nm, $\lambda_{em,max}$ = 560 nm) and with an average diameter of 0.84 µm were used. They were diluted with a Fluoresceine solution (150 µmol/l) in a ratio of 1:8 to 1:12.

After generation of slug flow, the XY translation table of the microscope was manually synchronised with the slug motion thus maintains a constant position of the slug in the screen window. The screen window was then observed with the CCD camera at an x10 magnification (objective lens NA = 0.3) and the video sequence was recorded with the help of a personal computer. Since the length of slug was exceeded the screen width, only part of the slug was recorded. The complete transversing of a paraffin plug through a whole screen width was recorded at a fixed capillary position in order to observe the velocity difference between the two slugs.

Video processing is an important step in the PIV measurement. The recorded videos were resolved into single frames and converted into greyscale pictures in Bitmap-format. These pictures were then processed with the aid of the software Dantec Dynamics® Multiphase ePIV (developed by the Chair of fluid mechanics, University of Dortmund) which determines the displacement vectors of each particle image by calculating a total sum correlation matrix. The maximum of this correlation matrix gives the maximal correlation of two frames for a certain displacement vector. The shape of the maximal peak of the correlation matrix indicates the

quality of the calculated results for the displacement vectors. The sharper the peak the fewer different values for the displacements are detected in a single interrogation area. All results were analysed using the above correlation matrix.

CFD Particle Tracing

It is difficult to carry out experiments at all operating condition, thus a suitable methodology must be developed. We therefore used a method capable of calculating and visualising the convection resulting from a given stationary or non-stationary flow called CFD particle tracing. This converts an Eulerian description of a flow into the corresponding Lagrangian description at selected particle location. Practically we define some particle sources that generate virtual massless particles once or on a regular basis which follow the path in the given flow field over time.

We have developed an algorithm called GMVPT (General Mesh Viewer Particle Tracing) which does not carry out its own flow simulation, but imports flow fields from a series of CFD output files. The domain description is given by a coarse grid and can be refined down to the level of CFD refinement. These refinement levels are used to build up a hierarchical searching structure to determine in which cell each particle resides. Initially we define the position of a particle or particles and velocity. However, in most of the cases the velocity at the particle position chosen is not known and it has to be interpolated from the values at the grid nodes. So from the nodal information and the time step, we could determine the new position using the following simple relation:

$$\tilde{Z} = Z + \Delta t . V_P \qquad (5)$$

First we have to determine the cell in which the particle resided and which node data we have to use for the interpolation. This was done by using the multilevel structure of the grids as

shown in Figure 3. Ideally, full searches were made only at the coarse grid level and then only for the cells that were generated by refinement. However, this only works with cell hierarchies which have the property that all generated cells are included in the cells they are generated from. For boundary cells this is not always true. Due to this, the cells which are outside of their parent cell have to be checked separately at each refinement level. For complicated domains with complex coarse grids, this method sacrifices some information and it is therefore planned to replace this method at a later date by a quad tree based approach.

The CFD simulations were carried out for a system shown in Figure 1a. Each slug was considered separately as a two-dimensional, single phase domain and solved individually as a decoupled system. The length of the aqueous phase domain with and without film was assumed to be the same while the radius was modified with film thickness for aqueous slug with film. For organic slugs without film, the domain was considered as a closed geometry whereas with film there was inlet and outlet flow via the wall film. The front and rear interface of all slugs was assumed to be symmetric at all flow velocities even with the convective flow in or out of the organic slug via the film. The in-house developed open-source Finite Element CFD tool, FEATFLOW, was used for simulations. This package solves the following unsteady-state incompressible Navier-Stokes equation with velocity constraints by projected and coupled approach (Turek[26]).

$$\nabla \bullet u = 0,\ u_t - v\Delta u + u \bullet \nabla u + \nabla p = f, \qquad in\ \Omega \times [0,T] \tag{6}$$

In this study, the geometry considered is shown in Figure 1b, with front interface being concave and the rear interface convex for the aqueous slug and vice-a-versa for the organic slug. The structured two-dimensional coarse grid was generated with the help of in-house developed Design and Visualisation Software Resource (DeViSoR 2.1). The grid was refined near the wall and corner of the geometry to improve the resolution. The Dirichlet type

boundary conditions were used for the aqueous slug with and without film. The same boundary conditions were used for the organic slug without film as well since there was no inflow and outflow. For organic phase domain with film i.e. with film inlet and outlet flows, Neumann type boundary conditions were used. A negative x-velocity was given to the capillary wall which moved the capillary wall in negative direction while the slug remained stationary. The other parameters were defined relative to the slug velocity according to domain requirement.

The simulations for particle tracing were carried out with the result obtained from CFD simulations. The meshes with different levels of refinement were generated with the help of the in-house developed graphical pre-processing tool, TRIGEN2D, a tool for two-dimensional coarse triangulations and to write the corresponding data in special format onto a hard disc. We inserted a rectangular area of tracers with a constant frequency to simulate a constant stream of particles at various operating conditions.

Results and Discussion

PIV

The experimental snapshot of fluorescence particles with PIV investigations in terms of velocity vectors for three different average velocities is shown in Figure 4. The experimental PIV measurements were carried out at very low flow rates due to experimental limitations while CFD simulations were carried out to study internal circulations over a wide operating window. In the PIV illustration of the velocity vectors, the green field indicates the correlation is good agreement whereas the red background indicates less satisfactory correlation peaks. For the comparison of the vector fields it should be noted that the velocity vectors have been scaled differently in the illustrations presented.

It can be seen from Figure 4 that the velocity of the back-flow increases in the vicinity of capillary wall relative to the flow rate close to the capillary symmetry axis. At the average flow velocity of 0.031 mm/s, particles in the vicinity of the wall flow in the reverse direction, but back-flow only occurs to a very limited extent. With increasing flow velocity to 0.072 mm/s, the back-flow of particles is not strongly pronounced. The illustration shows a similar relative velocity vector field. In the third PIV snapshot (Vav = 0.086 mm/s), one can observe internal circulations at the front end clearly while the rear interface is not visible. This shows that at extremely low flow velocities the particles are stagnant and start circulating over the slug length with increase in the flow velocity. Several videos were taken sequentially during this experimental study. It was observed that the wall film provides lubricating action to enclosed slug, whereby the slug surrounded by film moves with higher speed as compared to the average velocity.

CFD Simulations

In the capillary slug flow reactor, when the solute diffuses through the interface from one slug to another, it subsequently circulates within the slug. The solute moves towards the front end of the slug, part of it is retained in a quiescent zone at the front end, while the remainder recalculates along the wall to the centre of the slug at the rear end. Convective mass transfer takes place to a degree depending on the intensity of internal circulation, while interphase mass transfer depends on the intensity of flow at the end of both slugs. This recirculation is characterised by a recirculation time and recirculation patterns ascertained with the help of CFD simulations without mass transfer. The contours of the internal circulations (velocity vector magnitude) within the aqueous and organic slug indicating circulation patterns and stagnant zones (zero vector magnitude) are shown in Figure 5. These circulations were observed at all flow velocities comparison with PIV experiments. This discrepancy with the PIV results is probably due to particle inertia. Analogous to this study, Handique and Burns[27]

presented recirculation inside the discrete liquid drop in a slit type microreactor and studied the convection and diffusion dominated mixing behaviour of solute in a discrete moving drop.

The liquid circulates around the two stagnant zones (see Figure 1b) showing a more intense recirculation at the centre of the slug and in between the two stagnant zones. In the stagnant zones the velocity is zero and the radial position was calculated by equating u(r) equal to zero in the velocity profile equation. This radial position shows the area of available for upstream and downstream flows during recirculation. The dimensionless radial distance as a function of average flow velocity is plotted in Figure 6. As can be seen, for slugs with length greater than their diameter, the radial position (r^0/R_s) is located at roughly half the capillary radius and shifts slightly towards the centre of the slug with increasing liquid flow velocity. On the other hand, in the case of shorter slugs (i.e. organic slug L = 0.561 mm) the dimensionless radial position is 0.72 at low velocity and with increasing flow velocity the radial position diminishes rapidly, approaching 0.5 at 200 mm/s. The distance of the stagnant zone from the rear interface (x/L) indicating symmetry of the circulation, was also predicted from the simulated results and plotted in Figure 7. At low flow velocities, the stagnant zone is at half of the length of the slug and with increasing velocity (~50 mm/s) the stagnant zone shifts towards the rear interface of the slug. In this case liquid circulates around the stagnant zone and exhibits intense circulation at the rear interface. For the slugs without film, with increasing length of the slug, the stagnant zone shifts more towards the rear side end of the slug. The same behaviour was also observed for an aqueous slug with film. In the case of the organic slug with a wall film, since there is inflow and outflow, the stagnant zone is at the centre of the slug at all flow velocities, and the intensity of recirculation is maximum at the centre line.

The average circulation time within the slug is calculated from simulated results (Equation 3 and 4) and plotted as a function of average flow velocities in Figure 8. Thulasidas et al[14] reported recirculation time in gas-liquid flow with film and showed that at low capillary numbers the recirculation time inside the liquid slug is constant but increases at high capillary number (~ 0.1). In case of a slug without film, for a slug of sufficient length (L>D), the flow velocity has no significant effect on normalised circulation time. The dimensionless circulation time varies between 3 and 4, which indicate that a typical element inside the slug will move from one end of the slug to other end during the time the slug travel a distance 3 to 4 times its own length. For a slug with a length less than its diameter (e.g. organic slug with L = 0.5616 mm in Figure 8), at low liquid velocity the circulation time was constant, but with increasing the flow velocity, circulation time decreases and subsequently remains constant. This indicates that at low flow velocity, the liquid circulates slowly and the circulation rate is enhanced with increasing flow velocity above 80 mm/s but further increases in velocity has no effect on recirculation time. With a wall film, for the aqueous slug the circulation time is slightly larger than the case of without film due to the decrease in the diameter of the slug and increase in slug velocity. It also decreases with increase in the flow velocity. For the organic slug, the circulation time is constant at all flow velocities due to wall film inflow and outflow. This information on the behaviour internal circulation patterns and circulation time might be used in surface renewal model to calculate the mass transfer.

Particle Tracing

Simulations were carried out with 2000 macro time steps and duration of 0.01 for both the slugs at different tracer block locations. The internal circulations inside aqueous and organic slugs using particle tracing observed at different times for a flow velocity of 5.64 mm/s are shown in Figure 9. As can be seen, at time zero a square block with 100x100 particles was introduced on the axis near the rear interface. With increasing time, the particles are swept

along with the flow and reach the front end of the slug with a approximate time of 2.5 sec (normalised time, 2.95) for aqueous slug and 1 sec for organic slug. Many particle tracing simulations were carried out with different particle blocks for all slugs. The simulations with blocks of height equal to the diameter of the slug clearly show the circulations and the stagnant zone inside the slug. The particles in the stagnant zone remain at the same position while the other particles move around them due to recirculation. During recirculation some particles tend to remain at the front end of the slug even at finer level of mesh refinement. This seems to depend on the curvature of interface, which is function of surface tension properties. This information is useful in the design of a capillary slug flow microreactor in order to induce suitable internal circulations. Thus, the particle tracing provides a quantitatively good prediction of internal circulations inside the liquid slugs.

Conclusion

The experiments were carried out using PIV technique and the effect of different flow velocities on internal circulations has been studied with the help of CFD. A particle tracing algorithm was developed to visualise the flow patterns inside the slug. The PIV experiments show qualitatively reliable circulations at low flow velocities. The simulated results show that the position of the stagnant zone changes with changing flow velocity. At low flow velocities and for slug with sufficient length, the flow has no significant effect on the circulation time inside the slug but with increasing in flow velocity the circulation time decreases. The simulations reveal a slightly but important effect of the presence of a wall film on the circulation patterns and rates. The particle tracing algorithm developed yields qualitative and quantitative information about the circulations and stagnant zones. In the future work, free surface CFD methodology will be developed and further experiments will be carried out to determine details of internal circulations.

Notations

C_a	Capillary number [-]
h	Film thickness [mm]
L	Length of slug [mm]
R	Radius of capillary [mm]
R_S	Radius of slug [mm]
r	Radial position [mm]
r^0	Radial position of stagnant zone [mm]
$U(r)$	Velocity inside the slug at radial position r [mm/s]
V_{av}	Average flow velocity [mm/s]
V_S	Slug velocity [mm/s]
V_P	Velocity of particle [mm/s]
t	Circulation time [-]
x	Distance of stagnant zone from rear interface, mm
Z	Initial position of the particle [mm]
$\tilde{Z}$	Position of particle after time Δt [mm]

References

1) Burns, J. R.; Ramshaw, C. The intensification of rapid reactions in multiphase systems using slug flow in capillaries. *Lab on Chips.*, **2001**, *1, 10-15.*
2) Dummann Gerrit; Quittmenn Ulrich; Gröschel Lother; Agar David, W.; Wörz Otto; Morgenschweis Konard. The capillary-microreactor: a new reactor concept for the intensification of heat and mass transfer in liquid-liquid reactions, *Catal. Today*, **2003**, *79-80, 433-439.*
3) Paglianti, A.; Giona, M.; Soldati, A. Characterization of subregimes in two-phase slug flow, *Int. J. Multiphase Flow*, **1996**, *22 (4), 783-796.*
4) Mishima K.; Hibiki T. Some characteristics of air-water two-phase flow in small diameter vertical tubes, *Int. J. Multiphase Flow*, **1996,** *22, 703–712.*
5) Triplett, K. A.; Ghiaasiaan, S. M.; Abdel-Khalik, S. I.; Sadowski, D. L. Gas-Liquid two-phase flow in microchannels Part I: two-phase flow patterns. *Int. J. Multiphase Flow*, **1999**, *25, 377-394.*
6) Kreutzer Michiel. Hydrodynamics of Taylor flows in capillaries and monolith reactors, *Ph.D Thesis, Delft University Press, Netherlands,* **2003**.
7) Simmons, M.J.; Wong, D.C.Y.; Travers, P.J.; Rothwell J.S. Bubble behaviour in three phase capillary microreactors. *Int. J. Chem. Reactor Eng.*, **2003**, *1, A (30).*
8) Thulasidas, T.C; Abraham, M. A.; Cerro, R. L. Bubble train flow in capillaries of circular and square cross section. *Chem. Eng. Sci.*, **1995**, *50 (2), 183-199.*
9) Bercic Gorazd; Pinter Albin. The role of gas bubbles and liquid slug lengths on mass transport in the Taylor flow through capillaries, *Chem. Eng. Sci.*, **1997**, *52 (21/22), 3709-3719.*
10) Elperin, T.; Fominykh, A. Mass transfer during gas absorption in a vertical gas liquid slug flow with small bubbles in liquid plugs, *Heat Mass Transfer*,**1998**, *33, 489-494.*

11) Van Baten, J. M.; Krishna R. CFD simulations of mass transfer from Taylor bubbles rising in circular capillaries, *Chem. Eng. Sci*., **2004**, *59, 2535 – 2545.*

12) Meinhart, C. D.; Wereley, S. T.; Gray, H. B. Volume illumination for two-dimensional particle image velocimetry, *Meas. Sci. Technol.*, **2000**, *11, 809-814.*

13) Pan, C. T.; Chuang, H. S.; Cheng, C. Y.; Yang, C. T. Micro-flow measurement with a laser diode micro-particle image velocimetry. *Sensors & Actuators A*, **2004**, *116, 51-58.*

14) Thulasidas, T.C.; Abraham, M. A.; Cerro, R. L. Flow pattern in liquid slugs during bubble train flow inside capillaries. *Chem. Eng. Sci.*, **1997**, *52 (17), 2947-2962.*

15) Piarah, W. H.; Paschedag, A.; Kraume, M. Numerical simulation of mass transfer between a single drop and an ambient flow. *AIChE J.*, **2001**, *47 (7), 1701-1704.*

16) Waheed Adekojo, M.; Henschke Martin; Pfennig Andreas (2002). Mass transfer by free and forced convection from single spherical liquid drops. *Int. J. Heat Mass Transfer*, **2002**, *45, 4507-4514.*

17) Bothe Dieter.; Koebe Mario.; Wielage Kerstin; Warnecke Hans-Joachim. VOF-simulations of mass transfer from single bubbles and bubble chains rising in aqueous solutions, *Proceedings of FEDSM'03: 4th ASME_JSME Joint Fluids Engineering Conference, Honolulu, Hawaii, USA*, **2003**.

18) Taha, T.; Cui, Z. F. Hydrodynamics of slug flow inside the capillaries. *Chem. Eng. Sci.*, **2004**, *59, 1181-1190.*

19) Hodgson, G. W. ; Charles, M. E. The pipeline flow of capsules, Part 1: Theoretical analysis of the concentric flow of cylindrical forms, *Can. J. Chem. Eng.*, **1963,** *43-45.*

20) Charles, M. E. The pipeline flow of capsules, Part 2: The concept of capsule pipelining. *Can. J. Chem. Eng.*, **1963**, *46-51.*

21) Harries, N.; Burns, J. R.; Barrow, D. A.; Ramshaw, C. A numerical model for segmented flow in a microreactor, *Int. J. Heat Mass Transfer*, **2003**, *46, 3313-3322.*

22) Ranade Vivek, V. Computational flow modelling for chemical rector engineering, Academic Press, London, **2000**.

23) Jiang, Y.; Khadilkar, M. R.; Al-Dahhan, M. H. and Dudukovic, M. P. CFD of Multiphase Flow in Packed-Bed Reactors: *AIChE J.*, **2002**, *48 (4), 701-715.*

24) Gruber Rainer, Radial mass transfer enhancement in bubble train flow, *Ph.D. Thesis, RWTH Aachen, Germany,* **2001**.

25) Bico, J.; Quere, D. Liquid trains in a tube, *Europhysics Letters,* **2000***, 51(5), 546-550.*

26) Turek, S. Efficient Solvers for Incompressible Flow Problems: An Algorithmic and Computational Approach, Springer-Verlag, Heidelberg, **1999**.

27) Handique, K.; Burns, M. A. Mathematical modelling of drop mixing in a slit type microchannel. *J. Micromech. Microeng.,* **2001**, *11, 548-554.*

List of Figures

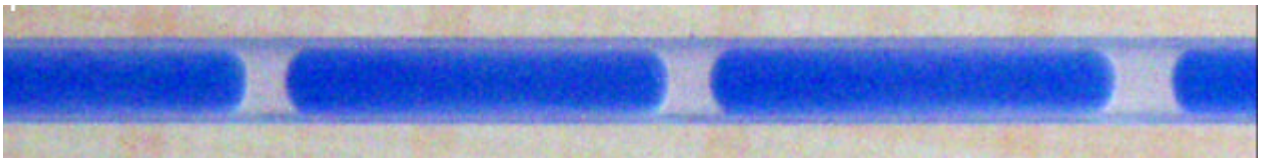

Figure 1a. Liquid-liquid slug flow in a capillary microreactor showing alternate long water (aqueous) and colourless cyclohexane (organic) slug

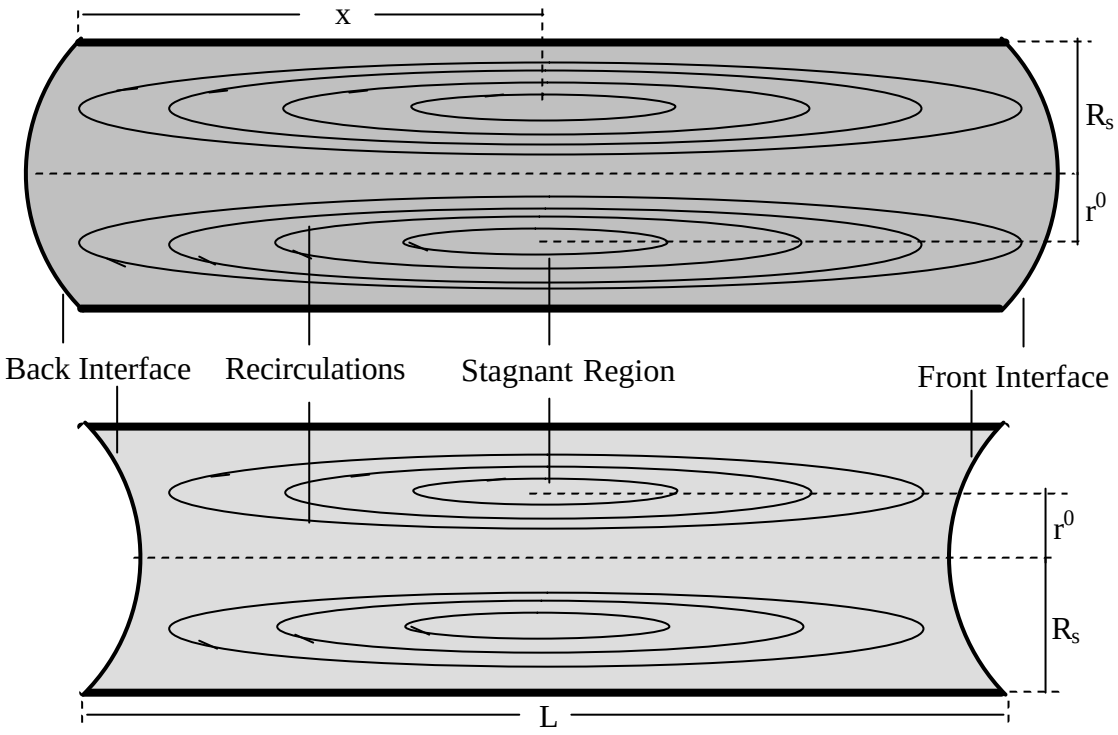

Figure 1b. Schematic representation of internal circulations inside the aqueous and organic slug respectively

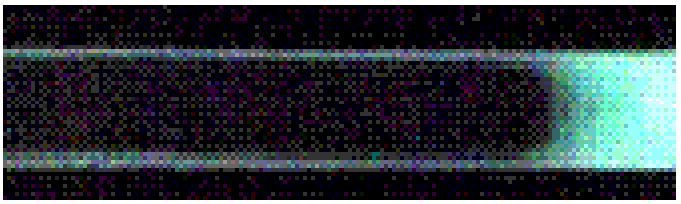

Figure 1c. Liquid-liquid slug flow of water (with fluorescence) – paraffin oil clearly showing the formation of paraffin oil film.

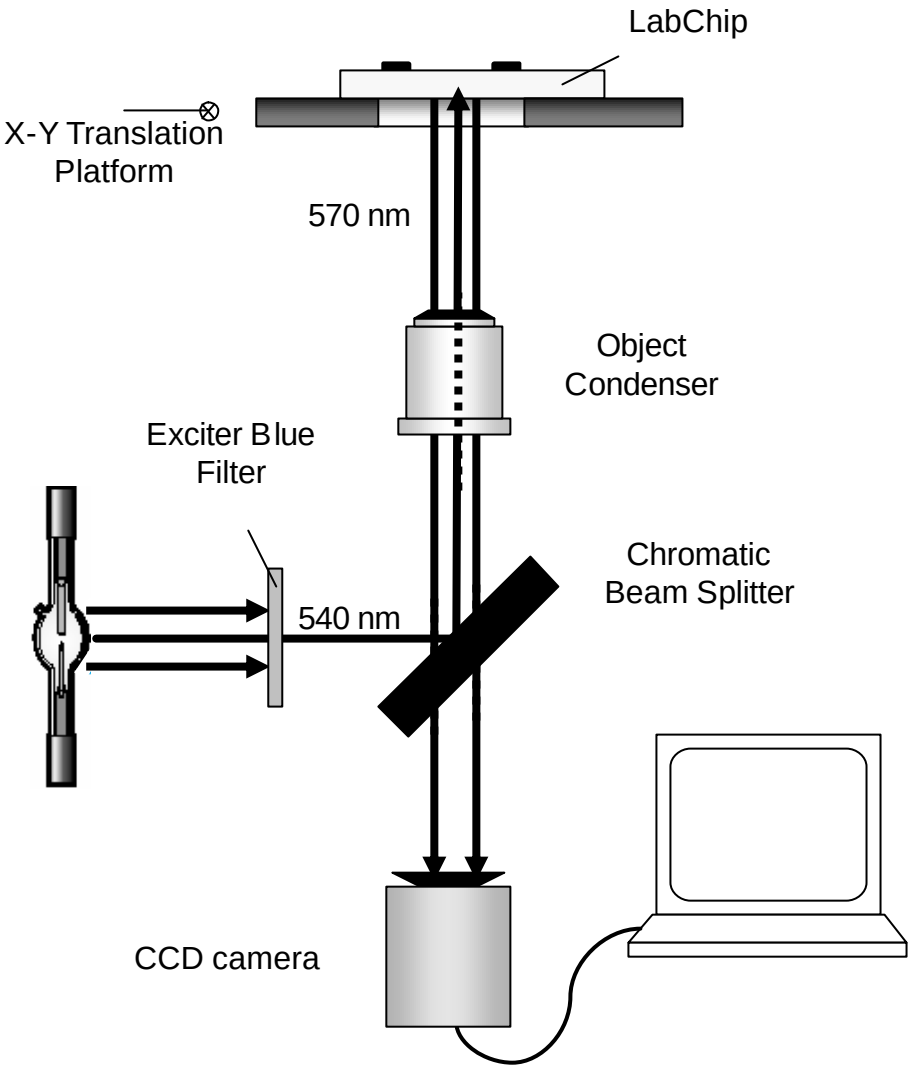

Figure 2. Experimental set up for PIV measurement

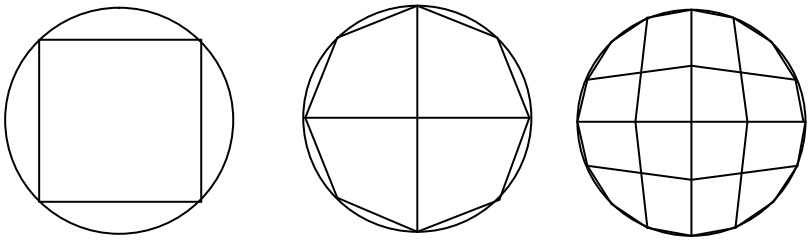

Figure 3. Cell refinement

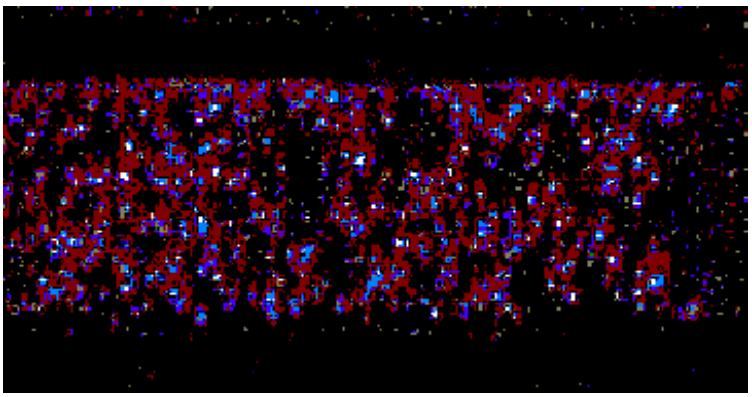

Vav = 0.031 mm/s

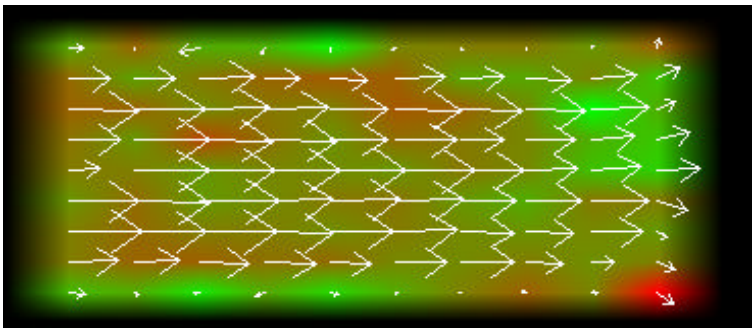

Vav = 0.031 mm/s

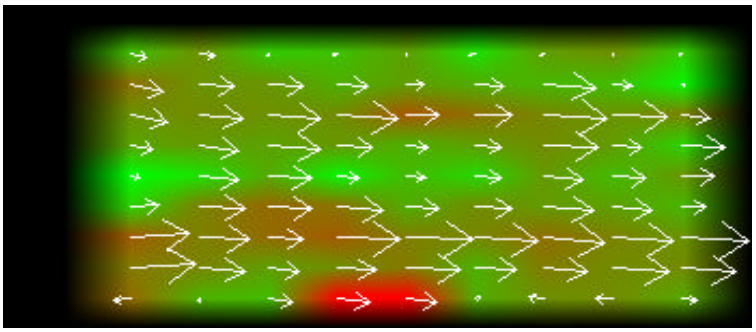

Vav = 0.072 mm/s

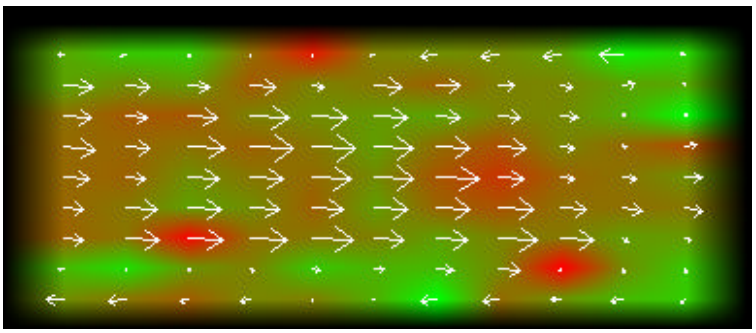

Vav = 0.086 mm/s

Figure 4. Experimental snapshot and PIV velocity distribution within the slug

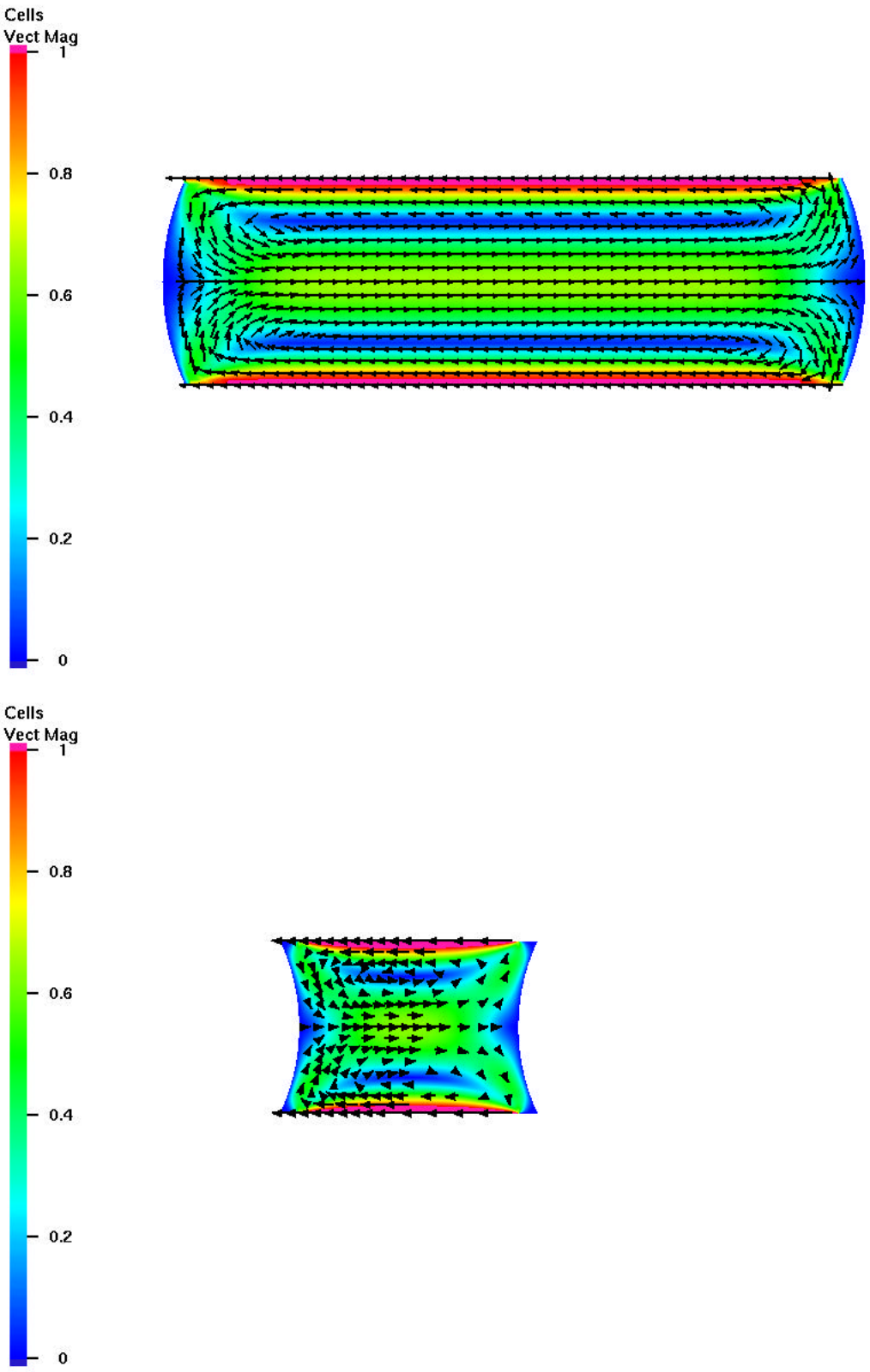

Figure 5. CFD simulated internal circulations within an aqueous and an organic slug respectively

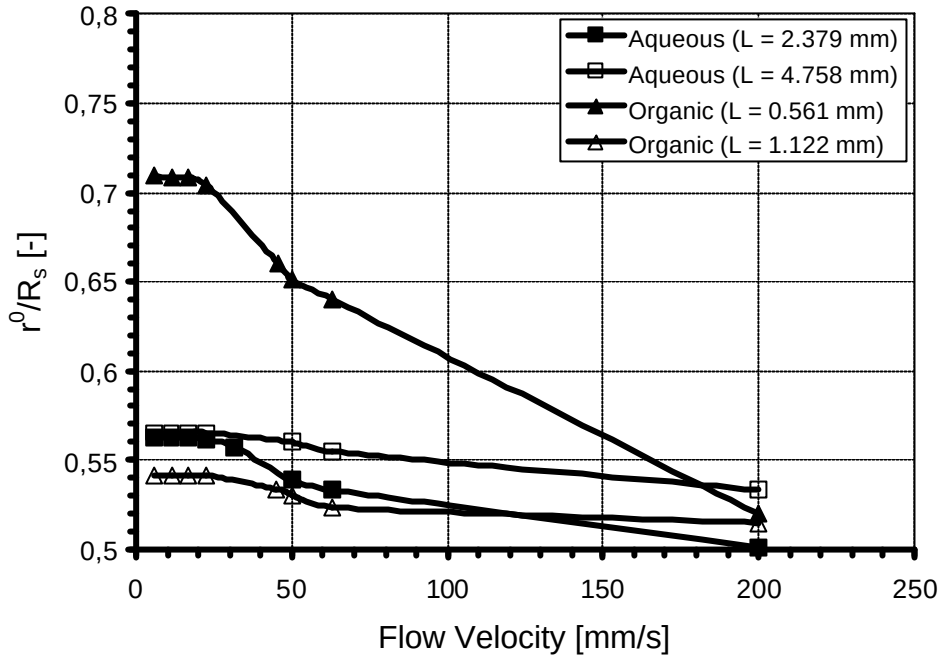

(a)

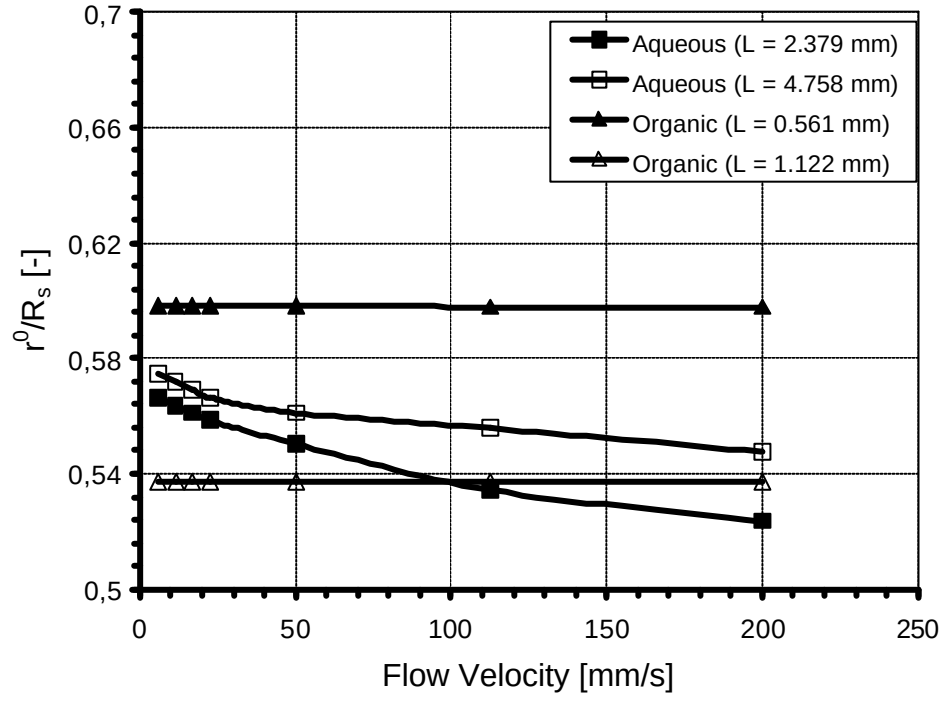

(b)

Figure 6: Radial position of stagnant region within the slug (a) without film and (b) with film.

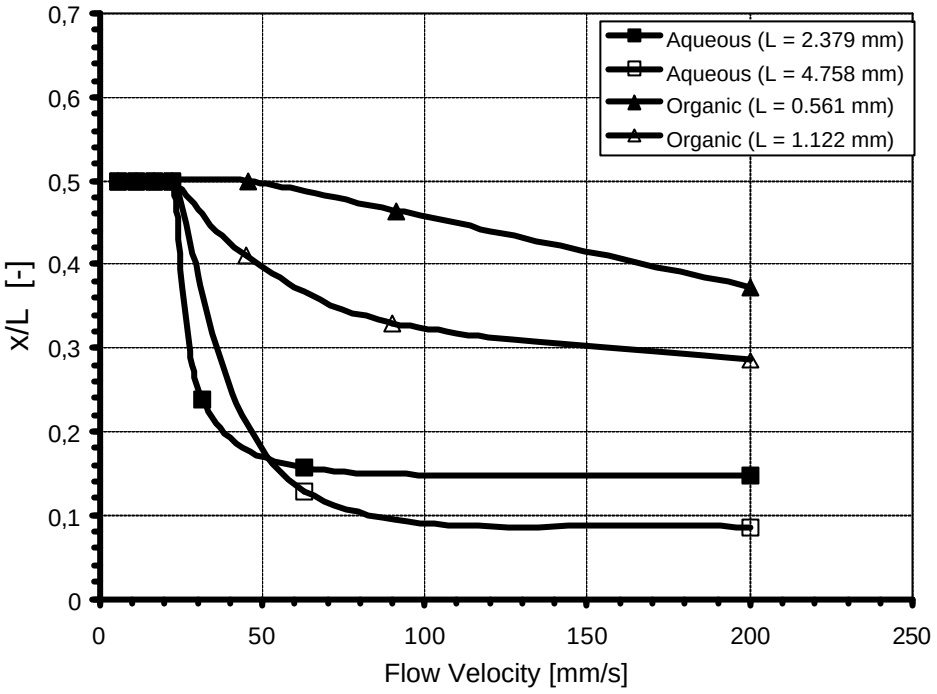

(a)

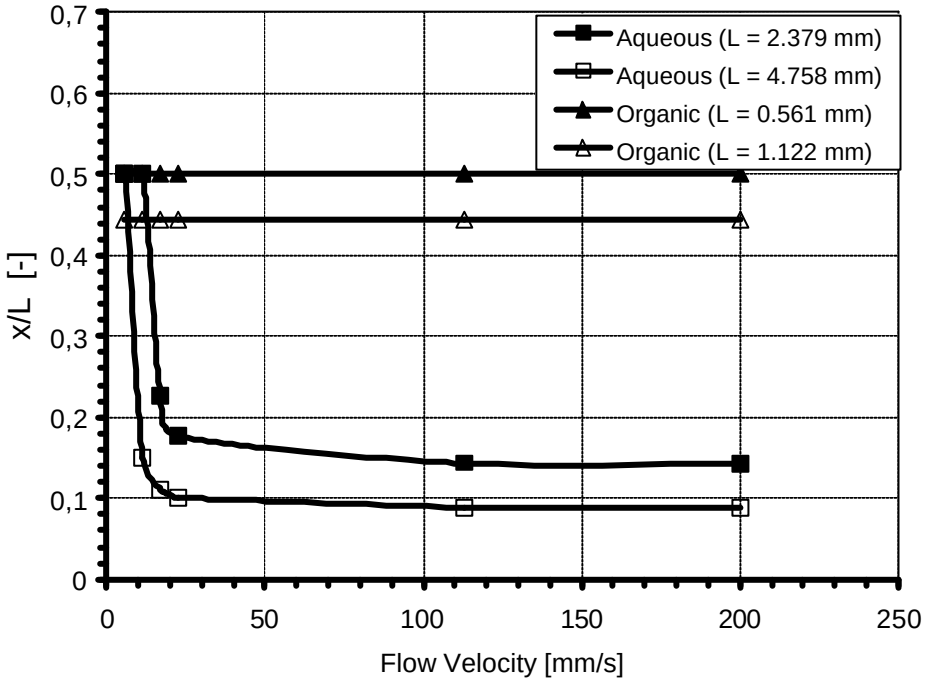

(b)

Figure 7: Distance of stagnant region centre from the back interface (a) without film and (b) with film.

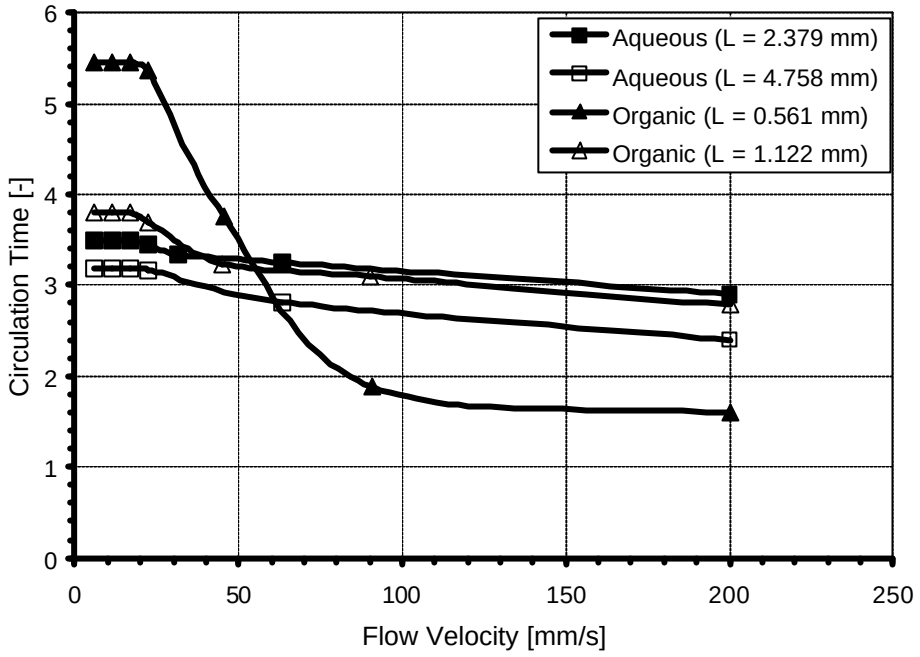

(a)

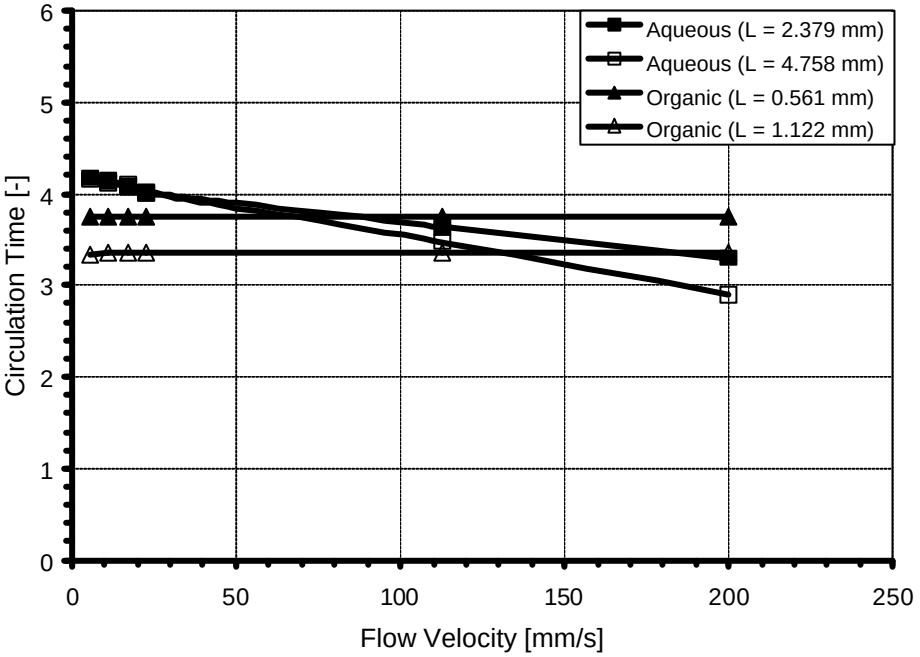

(b)

Figure 8. Circulation time within the liquid slug (a) without film and (b) with film

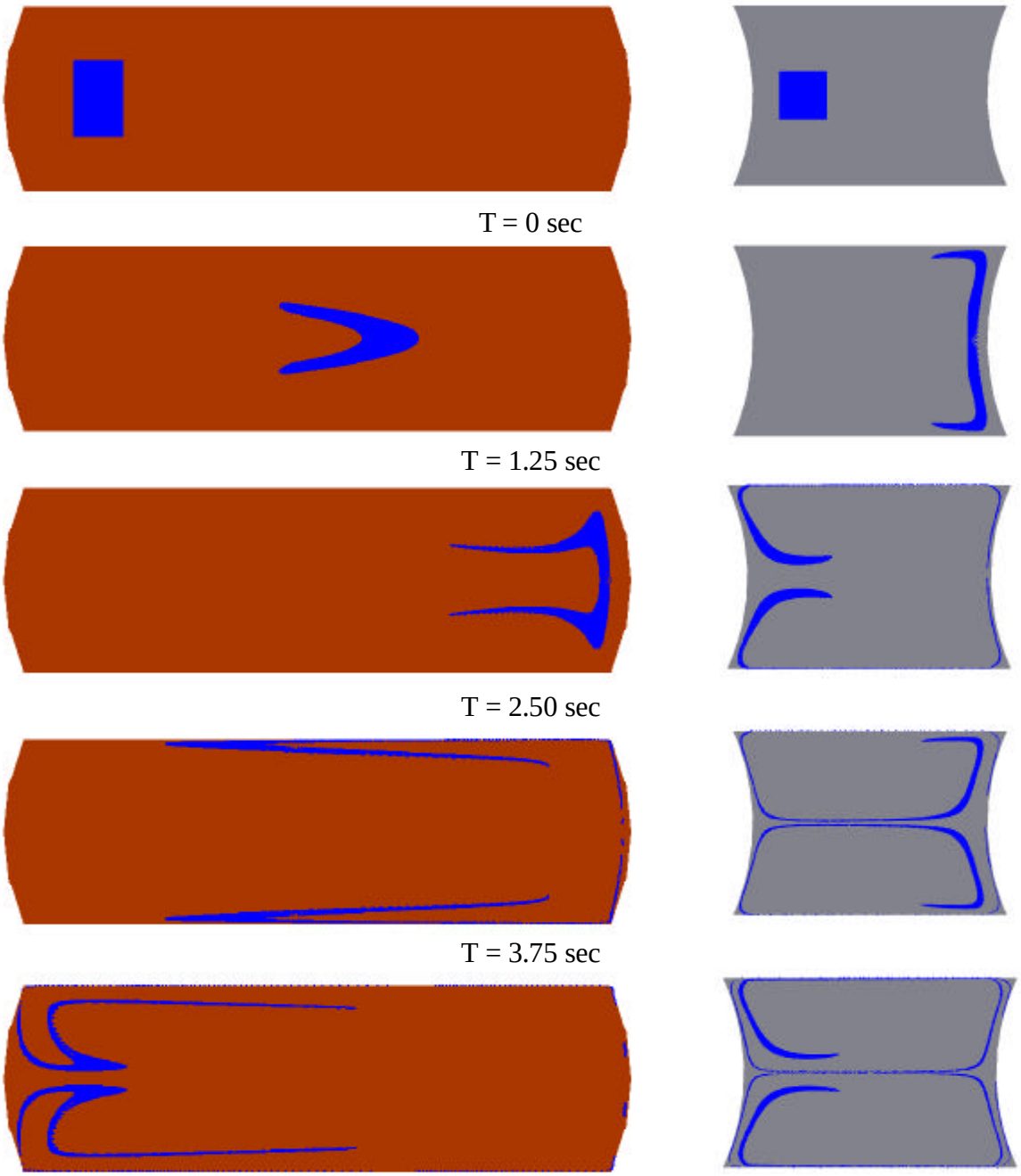

Figure 9. Internal circulations by particle tracing in aqueous and organic slugs respectively.
(V_{av} = 5.64 mm/s, D = 0.75 mm)